



Published in final edited form as:

*Nat Chem Biol.* 2019 May ; 15(5): 480–488. doi:10.1038/s41589-019-0249-y.

## Molybdenum cofactor transfer from bacteria to nematode mediates sulfite detoxification

Kurt Warnhoff<sup>1</sup> and Gary Ruvkun<sup>1</sup>

<sup>1</sup>) Department of Molecular Biology, Massachusetts General Hospital, Boston, MA 02114

### Abstract

The kingdoms of life share many small molecule cofactors and coenzymes. Molybdenum cofactor (Moco) is synthesized by many archaea, bacteria, and eukaryotes, and is essential for human viability. The genome of the animal *Caenorhabditis elegans* contains all of the Moco biosynthesis genes, and surprisingly these genes are not essential if animals are fed a bacterial diet that synthesizes Moco. *C. elegans* lacking both endogenous Moco synthesis and dietary Moco from bacteria arrest development, demonstrating interkingdom Moco transfer. Our screen of *E. coli* mutants identified genes necessary for synthesis of bacterial Moco or transfer to *C. elegans*. Moco-deficient *C. elegans* developmental arrest is caused by loss of sulfite oxidase, a Moco-requiring enzyme, and is suppressed by mutations in either *C. elegans* cystathionine gamma-lyase or cysteine dioxygenase, blocking toxic sulfite production from cystathionine. Thus, we define the genetic pathways for an interkingdom dialogue focused on sulfur homeostasis.

### Introduction:

Molybdenum cofactor (Moco) is a tricyclic pyranopterin with a coordinated molybdenum that is synthesized in multiple enzymatic steps from GTP (Fig. 1)<sup>1</sup>. Moco and the enzymes that synthesize Moco are conserved across archaea, bacteria, and eukarya<sup>2</sup>. The steps in Moco synthesis emerged from bacterial genetic analyses<sup>3</sup>. Human Moco deficiency causes seizures, progressive neurological damage, and neonatal death<sup>4,5</sup>. Moco is an essential cofactor for four animal enzymes; sulfite oxidase, xanthine oxidase, aldehyde oxidase, and the mitochondrial amidoxime reducing component<sup>4</sup>, but loss of sulfite oxidase activity is

Users may view, print, copy, and download text and data-mine the content in such documents, for the purposes of academic research, subject always to the full Conditions of use:[http://www.nature.com/authors/editorial\\_policies/license.html#terms](http://www.nature.com/authors/editorial_policies/license.html#terms)

Correspondence: [ruvkun@molbio.mgh.harvard.edu](mailto:ruvkun@molbio.mgh.harvard.edu).

Author Contributions:

K.W. and G.R. designed and K.W. performed experiments. K.W. and G.R. wrote manuscript.

Quantification and statistical analysis:

ImageJ was used for image analysis. GraphPad Prism software was used for calculations of IC50, median, upper, and lower quartiles. Sample size, dispersion, and precision measures are described in the figure legends. No data points were excluded from this study based off statistical tests.

Data Availability Statement:

Further information and reasonable requests for data, resources, sequences, and reagents should be directed to and will be fulfilled by the corresponding author.

Competing Interests:

The authors declare no competing interests.

suspected to be the primary pathology in human Moco deficiency<sup>1</sup>. Because Moco is unstable, it has not been thought to be transferred between cells, tissues, or organisms.

Here we show that *C. elegans* can acquire mature Moco and a Moco precursor (cPMP, cyclic pyranopterin monophosphate) from its bacterial diet. We show *C. elegans* lacking endogenous Moco synthesis and dietary Moco arrest development due to an inability to detoxify sulfite. *C. elegans* cystathionine gamma lyase and cysteine dioxygenase, conserved components of the sulfur amino acid catabolism pathway, generate sulfite that is lethal when Moco is deficient<sup>6</sup>. In the absence of sulfur amino acid catabolism, Moco is no longer necessary. Thus, interkingdom transport of Moco from microbes to *C. elegans* acts in sulfite detoxification.

## Results:

### Moco synthesis and dietary acquisition in *C. elegans*:

We explored the function of Moco and its biosynthetic enzymes in the animal *C. elegans*. Genome sequence analysis using protein queries from *E. coli* Moco biosynthesis enzymes identified *C. elegans* homologs for each of the 7 core Moco-biosynthesis proteins (Fig. 1A, Supplementary Table 1)<sup>1</sup>. We characterized phenotypes of *C. elegans* with loss-of-function mutations in six predicted Moco biosynthesis enzymes: *moc-1*, *moc-2*, *moc-3*, *moc-4* (T27A3.6), *moc-5* (F49E2.1), and *lin-46*<sup>7-9</sup>. Surprisingly, given that Moco biosynthesis is essential in humans, *C. elegans* strains carrying mutations in any of these genes were viable and grew normally on wild-type *E. coli*. We hypothesized that *C. elegans* acquires Moco from the *E. coli*, which is competent for Moco synthesis, on which it feeds. In the wild *C. elegans* consumes many different species of bacteria in rotting fruit. Because Moco biosynthesis is not universal to all bacteria, it is reasonable to expect *C. elegans* to import bacterial Moco as well as synthesize Moco *de novo*<sup>10</sup>. To test this hypothesis, we grew wild-type and Moco-biosynthesis mutant *C. elegans* strains on an *E. coli* strain with a deletion in MoaA, the first step in Moco biosynthesis. This MoaA *E. coli* strain, which grows at a normal rate on LB or nematode growth media (NGM), cannot synthesize Moco or any of the Moco precursor metabolites. Wild-type *C. elegans* grows normally feeding on MoaA *E. coli*, demonstrating that microbial Moco biosynthesis is not required for viability of wild-type *C. elegans* (Fig. 1B). *C. elegans* with a mutation in *moc-1*, *moc-2*, *moc-3*, *moc-4*, or *moc-5* arrested or died at early larval stages when grown on MoaA *E. coli*, in contrast to the healthy growth of these *C. elegans* mutants fed wild-type *E. coli* (Fig. 1B and Fig. 2A–F). Of the 6 putative *C. elegans* Moco-biosynthesis mutants tested, only the *lin-46* mutant grew normally on MoaA *E. coli* (Supplementary Fig. 1). LIN-46 and MOC-1 are paralogous, likely emerging from a MoeA duplication event. LIN-46 displays less sequence similarity to MoeA than MOC-1 (Supplementary Table 1), and thus may be functionally divergent. Mutations in *lin-46* emerged from studies of miRNA biology, and were not characterized further here<sup>7</sup>. We also found evidence for maternal contribution of Moco: when *moc-1*, *moc-2*, *moc-3*, *moc-4*, and *moc-5* mutant *C. elegans* mothers were fed MoaA *E. coli* from the L4 stage of development, one stage prior to reproductive adulthood, progeny viability dropped dramatically (Supplementary Table 2). Embryo viability was not affected

when wild-type mothers were fed wild-type or MoeA *E. coli*. Thus, our data suggests that Moco is transferred from mother to progeny.

We identify redundant pathways for maintaining sufficient Moco in *C. elegans*: endogenous Moco biosynthesis and acquisition from dietary *E. coli*. To test whether the ability of *E. coli* to synthesize Moco and transfer it to *C. elegans* is common in bacterial species associated with *C. elegans* in the wild, we examined the growth of *moc-1* mutant *C. elegans* cultured on 6 bacterial strains isolated from the natural *Caenorhabditis* microbiome<sup>10,11</sup>. *C. elegans moc-1* mutants grew and developed on all 6 natural bacterial isolates tested, representing 5 unique bacterial phyla (Fig. 1B, Supplementary Table 3). Thus diverse bacterial species from the natural *Caenorhabditis* habitat supply Moco to *C. elegans*, suggesting this is a conserved and robust host-microbe interaction. *C. elegans* may retain its Moco biosynthetic genes because not all bacterial species it naturally consumes synthesize Moco. Genome analyses showed that 325 out of 451 bacterial species carry Moco biosynthesis genes<sup>2</sup>. In eukaryotes, Moco biosynthetic genes are generally present, but particular fungal and protist species lack Moco biosynthesis.

### ***C. elegans* acquires microbial cPMP and Moco:**

To define the comprehensive set of *E. coli* gene activities that are required for the synthesis or transfer of Moco to *C. elegans*, we tested growth of the *moc-1* mutant animals on each of the approximately 4,000 mutant strains of the Keio *E. coli* deletion mutation collection<sup>12</sup>. We screened for *E. coli* mutant strains that permit growth of wild-type *C. elegans*, but not *moc-1* mutant animals. This screen identified 12 *E. coli* genes that are specifically required for the viability of *moc-1* mutant animals (Supplementary Fig. 2A). The genes identified include the 7 enzymes that synthesize Moco from GTP (MoaA/C/D/E, MoeA/B, and MogA). We also identified the *E. coli* ABC-type transport system for acquisition of environmental molybdenum for incorporation into Moco (ModA/B/C)<sup>13</sup>. Finally, we discovered 2 new *E. coli* genes that have no known function in Moco biosynthesis, YdaV and YehP.

Ten of the 12 *E. coli* mutations that disrupt the growth of *moc-1* mutant *C. elegans* disrupt steps in Moco biosynthesis. These data strongly suggest that Moco or biochemical precursors in the *E. coli* Moco biosynthetic pathway are acquired and utilized by *C. elegans*. We used a matrix of *E. coli* and *C. elegans* Moco biosynthetic mutant combinations to determine which molecules are transferred from *E. coli* to *C. elegans*. Keio collection kanamycin resistant insertion/deletion mutations are likely polar, down regulating the expression of downstream genes in the operon and precluding disruption of single biochemical steps in Moco synthesis (Supplementary Fig. 2B,C). To precisely analyze *E. coli* single gene disruptions, the mutations were rendered nonpolar via Flp recombinase-mediated removal of each kanamycin cassette<sup>14</sup>. Of the 12 *E. coli* mutant strains identified in our screen, we generated nonpolar versions of all but the ModB mutation. Of the 11 nonpolar mutant strains generated, all but YehP recapitulated the larval lethality of *moc-1* mutant *C. elegans*, consistent with the original polar Keio *E. coli* mutations. This result suggests that the downstream gene in the Yeh operon, YehQ, may also need to be inactive for *E. coli* to fail in Moco biosynthesis or transport (Supplementary Fig. 3A,B). We did not

further analyze this operon. The 10 other nonpolar *E. coli* mutations were further analyzed for their ability to support the growth and development of *C. elegans* mutants that harbor defects at defined points in Moco biosynthesis.

We challenged wild-type, *moc-1*, *moc-2*, *moc-3*, *moc-4*, or *moc-5* mutant *C. elegans* to grow on wild-type *E. coli*, or *E. coli* with nonpolar mutations in MoaA, MoaC, MoaD, MoaE, MoeA, MoeB, MogA, ModA, ModC, or YdaV (Fig. 2, Supplementary Fig. 3C–H). *C. elegans moc-1*, *moc-2*, *moc-3*, and *moc-4* mutant animals were viable only on wild-type *E. coli* able to synthesize mature Moco (Fig. 2). This suggests that *C. elegans* acquire Moco from their diet: *moc-1* mutant animals cannot utilize other Moco-precursors from bacteria to synthesize mature Moco, and the growth of *moc-2*, *moc-3*, and *moc-4* mutants is not rescued when their respective downstream Moco-metabolites (MPT, MPT-AMP) are available from bacteria (Fig. 2C–E). These data suggest that *moc-1*, *moc-2*, *moc-3*, and *moc-4* mutant animals grow and develop by acquiring mature Moco from *E. coli*.

In contrast, *moc-5* mutant *C. elegans* displayed little or no growth on MoaA or MoaC *E. coli*, but near wild-type growth on *E. coli* lacking MoaD, MoaE or MoeB (Fig. 2A,B). MoaD, MoaE, and MoeB mutant *E. coli* accumulate cPMP (Supplementary Fig. 2B)<sup>15</sup>. *moc-5* mutant *C. elegans* is unable to make its own cPMP, but possess all of the downstream machinery to utilize cPMP to synthesize mature Moco. Thus, these genetic data suggest that cPMP provided by the MoaD, MoaE or MoeB mutant *E. coli* is bioavailable and supports the growth of *moc-5* mutant animals deficient in the production of cPMP. MogA and MoeA mutant *E. coli* also synthesize cPMP. Why do they not support the growth and development of *moc-5* mutant worms as well as MoaD, MoaE, and MoeB mutant *E. coli* (Fig. 2B)? We speculate that cPMP does not accumulate in MogA and MoeA mutant *E. coli* because they possess the enzymes that convert cPMP to MPT or MPT-AMP, respectively.

What form of Moco is taken up by *C. elegans* from *E. coli*? While animals utilize the di-oxo form of Moco (referred to as ‘Moco’ in this manuscript), the majority of *E. coli* molybdenum-utilizing enzymes are in the DMSO reductase family that utilizes bis-MGD Moco. This dinucleotide Moco variant is not utilized by eukaryotes and requires the activity of the MobA enzyme for its synthesis in *E. coli* (Supplementary Fig. 2B)<sup>16</sup>. To test whether the bis-MGD form of Moco is transferred from *E. coli* to *C. elegans*, we tested the ability of *moc-1* mutant *C. elegans* to grow on MobA *E. coli*. *moc-1* mutant animals grew normally on MobA bacteria (Fig. 1C), supporting the model that di-oxo Moco and not bis-MGD Moco is transferred from *E. coli* to *C. elegans*.

To further test whether the mature Moco prosthetic group is transferred from *E. coli* to *C. elegans*, we utilized the *E. coli* Mod mutants identified in our screen for inviable *moc-1* mutant *C. elegans*. The *E. coli* Mod operon encodes proteins necessary for molybdate import and thus biosynthesis of the molybdenum cofactor. Mod mutant *E. coli* fail to synthesize Moco when grown in standard culture media, but synthesize Moco when grown in media supplemented with 100µM molybdate<sup>17</sup>. Thus, Moco synthesis can be controlled in Mod mutant *E. coli* with molybdate supplementation. We cultured ModA and ModC mutant *E. coli* with and without 100µM supplemental molybdate and fed these bacteria to *moc-1* mutant *C. elegans*. Only when grown with supplemental molybdate do ModA or ModC

mutant *E. coli* support the growth of *moc-1* mutant *C. elegans* (Fig. 1C,D). No other *E. coli* mutants displayed this molybdate suppression (Fig. 1D).

An alternate explanation for the ability of wild-type *E. coli* to support the growth of *moc-1* mutant *C. elegans* is that the animal imports the gene products (mRNA or protein) of the bacterial Moco-biosynthesis enzymes. To exclude this possibility, we cultured *moc-1* mutant *C. elegans* on a 1:1 mixture of nonpolar MoaA and MoaD deletion *E. coli* strains. Neither of these strains individually supports the growth of *moc-1* mutant animals (Fig. 1C), yet the dietary combination of MoaA and MoaD bacterial strains possess all of the genes necessary for Moco biosynthesis. The MoaA + MoaD mixture caused larval arrest similar to either individual strain, suggesting that the complete set of *E. coli* Moco-biosynthetic mRNAs or enzymes present in the combination of the mutant bacterial strains are not transferred to complement *C. elegans* Moco deficiency (Fig. 1C). Rather, our data support a model that the Moco prosthetic group and cPMP produced by *E. coli* cells is transferred to *C. elegans*.

The *C. elegans* MOC-1 protein is homologous to bacterial and mammalian enzymes that insert molybdenum into MPT-AMP to synthesize mature Moco. We tested if the requirement for this enzyme could also be suppressed by high levels of molybdate. Indeed, *moc-1* mutant animals grown on MoaA mutant *E. coli* supplemented with 5mM molybdate partially bypass the requirement for MOC-1 in the synthesis of Moco (Supplementary Fig. 4).

#### **Moco-deficient phenotypes are promoted by CTH-2 and CDO-1:**

To better understand why *C. elegans* lacking endogenous and dietary Moco are not viable, we sought genetic suppressors of this lethality. We EMS-mutagenized populations of *moc-2*, *moc-3*, and *moc-4* *C. elegans* mutants and grew them on wild-type *E. coli* until the F2 generation. We then challenged the F2 generation animals to grow on MoaA *E. coli*, which normally causes completely penetrant larval arrest (Fig. 2). We identified 49 independent mutant strains that grew robustly and reproduced in the absence of Moco (Supplementary Table 4). To determine the causative genetic lesions in these mutants, DNA from each strain was analyzed via whole genome sequencing<sup>18</sup>. Based on the presence of multiple independent alleles, we identified mutations in two different genes that allow the viability of Moco-deficient *C. elegans* cultured on Moco-deficient *E. coli*. A mutation in either of these 2 genes was present in all 49 of the strains isolated in our screen.

We identified 45 alleles of the *C. elegans* cystathionine gamma-lyase, *cth-2*/ZK1127.10. These 45 alleles affected 37 distinct amino acid positions and included 9 nonsense and 36 missense mutations, suggesting that *cth-2* loss of function suppresses the growth arrest caused by *C. elegans* Moco deficiency (Fig. 3, Supplementary Table 4). Cystathionine gamma-lyase (CTH), an enzyme conserved across all kingdoms of life, catabolizes cystathionine into cysteine, ammonia, and  $\alpha$ -ketobutyrate, on the main axis of sulfur amino acid metabolism (Fig. 4A)<sup>6</sup>. To demonstrate the requirement of *cth-2* gene activity for the inviability of Moco-deficient *C. elegans* grown on Moco-deficient *E. coli*, we genetically transferred the *cth-2*(*mg599*) allele, predicted to cause a premature stop (W 21 Stop), into the *moc-1* mutant background and assayed growth and development. Like wild type, *cth-2* mutant animals grew well on both wild-type and MoaA *E. coli*. *moc-1* mutant animals grew well on wild-type *E. coli*, but displayed early larval arrest on MoaA *E. coli* (Fig. 3A).

*cth-2; moc-1* double mutant animals grew well on both wild-type and MoaA *E. coli* (Fig. 3A), demonstrating that the activity of *cth-2* is required for larval arrest caused by *C. elegans* Moco deficiency. *cth-2* is one of two cystathionine gamma-lyase-encoding genes in *C. elegans*. The CTH-1 protein, 86% identical to CTH-2, is not redundant with CTH-2 because only *cth-2* alleles emerged from this screen.

We also identified 4 alleles of *C. elegans* cysteine dioxygenase, *cdo-1*F56F10.3. We identified 3 missense mutations affecting conserved amino acids in the *cdo-1* active site and 1 nonsense mutation, suggesting that loss of function of *cdo-1* suppresses the growth arrest caused by *C. elegans* Moco deficiency (Fig. 3, Supplementary Table 4). Cysteine dioxygenase (CDO) acts immediately downstream of CTH-2 in the sulfur amino acid metabolism pathway, catalyzing the reaction of cysteine with dioxygen to generate cysteine sulfinate (Fig. 4)<sup>6</sup>. To demonstrate the requirement of *cdo-1* for the growth arrest of Moco-deficient *C. elegans*, we genetically transferred the *cdo-1*(*mg622*) allele (C85Y) into the *moc-1* mutant background and assayed growth and development. *cdo-1 moc-1* double mutant animals grew well on both wild-type and MoaA *E. coli*, recapitulating the suppression identified in our screen (Fig. 3A). Additionally, *cth-2* and *cdo-1* mutations suppressed embryogenesis defects caused by maternal Moco deficiency (Supplementary Table 2).

#### Sulfites inhibit development during Moco deficiency:

We hypothesized that CTH-2 and CDO-1-dependent catabolism of sulfur amino acids generates a product that is toxic if Moco is deficient. To test this idea, we treated animals with cysteine, a product of CTH-2 and a substrate for CDO-1, and tested for reversion of the *cth-2*(*lf*) or *cdo-1*(*lf*) suppression of Moco-deficient larval arrest on MoaA *E. coli* (Fig. 4A). Wild-type animals display half maximal growth rate (IC<sub>50</sub>) with 6.0mM cysteine. The *cth-2* mutant animals display an IC<sub>50</sub> of 8.4mM cysteine (Fig. 4B,C). In contrast, *cth-2; moc-1* double mutant animals are sensitive to cysteine (IC<sub>50</sub> 1.0mM cysteine); at 3mM cysteine *cth-2; moc-1* mutants arrest early in development (Fig. 4C,E). Thus *cth-2; moc-1* double mutant animals are 8 times more sensitive to cysteine than the *cth-2* single mutant, demonstrating that under Moco-deficient conditions, cysteine, a CTH-2 catabolic product, promotes larval arrest.

In contrast, *cdo-1* and *cdo-1 moc-1* mutant animals grew well on MoaA *E. coli* at most cysteine concentrations, displaying normal IC<sub>50</sub>s of 5.6mM and 4.1mM cysteine respectively (Fig. 4C,E). These results demonstrate that the activity of CDO-1 is required for the larval arrest caused by supplemental cysteine during Moco deficiency. To further explore the relationship between *cth-2*, *cdo-1*, and cysteine, we analyzed the growth of *cth-2; cdo-1 moc-1* triple mutant animals with cysteine. The *cth-2; cdo-1 moc-1* triple mutant (IC<sub>50</sub> of 3.1mM cysteine) displays growth on cysteine similar to *cdo-1 moc-1* (IC<sub>50</sub> of 4.0mM) double mutants and grows much better on cysteine than *cth-2; moc-1* double mutants (IC<sub>50</sub> of 0.4mM) (Fig. 4D,E). These data demonstrate that the function of *cdo-1* is epistatic to *cth-2* and cysteine supplementation and support the model that a cysteine catabolic product downstream of CDO-1 is responsible for the larval arrest caused by Moco deficiency.

Sulfites are produced via sulfur-amino acid catabolism downstream of both CTH-2 and CDO-1 (Fig. 4A). If cysteine-derived sulfites inhibit growth and development during Moco deficiency, supplemental sulfite should cause inviability independent of the activity of CTH-2 or CDO-1 during Moco deficiency. We cultured synchronized wild-type, *cth-2*, *cdo-1*, *cth-2*; *moc-1*, and *cdo-1 moc-1* mutant animals on Moco-deficient *E. coli* supplemented with sulfite and analyzed growth. When supplemented with 5mM sulfite, wild-type, *cth-2*, and *cdo-1* mutant animals display a slight developmental delay while *cth-2*; *moc-1* and *cdo-1 moc-1* double mutant animals arrest or die early in development (Fig. 4F). These data demonstrate that when animals are Moco deficient, sulfites cause developmental arrest independent both CTH-2 and CDO-1. We conclude that accumulation of sulfite generated by sulfur amino acid catabolism is toxic to *C. elegans* if animals are Moco deficient.

The previous experiments were all performed on animals fed *MoaA E. coli* eliminating contribution of dietary Moco. We wondered if dietary Moco could support *C. elegans* growth and development when animals are challenged with supplemental cysteine or sulfite. We assayed the growth of *moc-1* mutant *C. elegans* fed wild-type *E. coli*, competent for Moco synthesis, supplemented with 3mM cysteine or 5mM sulfite. Even when fed *E. coli* providing dietary Moco, *moc-1* mutant animals were sensitive to supplemental cysteine and sulfite when compared to wild-type animals (Supplementary Fig. 5). Thus, sufficient Moco to respond to environmental challenges to sulfur homeostasis cannot be derived from dietary sources alone.

#### Moco-deficient defects explained by loss SUOX-1 activity:

In animals, sulfite is oxidized to sulfate by the Moco-requiring enzyme, sulfite oxidase (*suox-1*/SUOX) (Fig. 4A). This reaction transfers electrons from sulfite to cytochrome C and the electron transport chain to generate sulfate, a proton gradient, and ATP<sup>19</sup>. Moco is also required for the function of 3 other animal enzymes; xanthine oxidoreductase, aldehyde oxidase, and mitochondrial amidoxime reducing component<sup>4</sup>. However, because the genetic suppressors of *C. elegans* Moco deficiency act in a pathway that produces sulfite, the pathology of *C. elegans* Moco deficiency is cleanly explained by a defect in sulfite oxidation. To test this model, we characterized *suox-1* null and hypomorphic mutations. We found that *suox-1* is an essential gene; *suox-1* null mutant animals display completely penetrant larval lethality (0% of *suox-1(mg663)* null mutant animals are viable (n=16) when grown on wild-type *E. coli*). Furthermore, the larval lethality of *suox-1* null mutant animals is suppressed by mutations in *cth-2* (90% of *cth-2(mg599)*; *suox-1(mg663)* animals were viable and fertile (n=19) when grown on wild-type *E. coli*). Thus, loss of *suox-1* phenocopies Moco-deficient phenotypes in *C. elegans*.

We also characterized *suox-1* missense mutations generated by the *C. elegans* Million Mutation Project (MMP) (Supplementary Table 5)<sup>20</sup>. One of the *suox-1* alleles analyzed, *suox-1(gk738847)* (D391N), grew normally on wild-type *E. coli*, but displayed a severe developmental delay when cultured on *MoaA E. coli* (Fig. 5A,B) and a reduced embryo viability when adult mothers were cultivated on Moco-deficient bacteria (Supplementary Table 2). Similar to Moco deficiency, these phenotypes were suppressed by loss of *cth-2* or

*cdo-1* (Fig. 5B, Supplementary Table 2). Thus, the activities of *cth-2* and *cdo-1* are necessary for the developmental defects caused by reduced SUOX-1 activity. These data suggest that SUOX-1 detoxifies the sulfite produced by sulfur amino acid catabolism. Consistent with this model, the *suox-1* hypomorphic mutant is hypersensitive to cysteine or sulfite, but not sulfate, (Fig. 5C–F). The phenotypic overlap between Moco deficiency and *suox-1(lf)* in *C. elegans* supports the model that the essential function of Moco is to maintain active sulfite oxidase protein and that Moco can either be synthesized in the animal cells or provided by the microbial diet.

### Tissue-specific rescue of *suox-1*, *moc-1*, and *cth-2*:

To determine in which tissues *C. elegans* SUOX-1 functions, we performed tissue-specific rescue experiments. The *suox-1* genomic locus was expressed under the control of the *rpl-28* (all tissues), *sng-1* (neurons), *vha-6* (intestine), *myo-3* (muscle), or *col-10* (hypodermis) tissue-specific promoters and tested for ability to rescue of the lethality of *suox-1(mg663)* null mutant animals. Transgenes expressing *suox-1* in all tissues or only in the hypodermis rescued the lethality of *suox-1(mg663)* animals (3/3 independent transgenic lines were viable for each transgene). In contrast, expression of *suox-1* in the neurons, muscle, or intestine failed to rescue the lethality of *suox-1(mg663)* (0/3 independent transgenic lines were viable for each of these transgenes). This suggests that the hypodermis is the primary site of *C. elegans* sulfite detoxification.

To determine the sites of MOC-1 activity, we performed similar tissue-specific rescue experiments. The *moc-1* genomic locus was expressed under the control of its native promoter, or the *sng-1* (neurons), *vha-6* (intestine), *myo-3* (muscle), or *col-10* (hypodermis) tissue-specific promoters. Multiple transgenic strains expressing *moc-1* under the control of these promoters were tested for their ability to rescue the larval arrest of *moc-1(ok366)* mutant animals grown on MoaA *E. coli*. Transgenes expressing *moc-1* under the control of its own promoter or the hypodermis-specific promoter rescued the larval arrest phenotype of *moc-1* mutant animals when grown on MoaA *E. coli* (Fig. 6A). The muscle-specific *Pmyo-3::MOC-1* transgene caused consistent rescue, although not as complete as *moc-1* driven by its own promoter or a hypodermal promoter (Fig. 6A). *moc-1* expression in neurons or the intestine did not rescue the inviability of *moc-1(ok366)* animals grown on MoaA *E. coli* (Fig. 6A). These data suggest that, similar to *suox-1*, the primary site of Moco biosynthesis is the *C. elegans* hypodermis. Distinct from *suox-1*, *C. elegans* muscle also appears to be a functional site of Moco synthesis via *moc-1* activity.

To determine the functional tissues of CTH-2 activity, we similarly expressed the *cth-2* genomic locus under the control of its native promoter or tissue-specific promoters. Multiple transgenic strains expressing *cth-2* under the control of these promoters were tested for their ability to promote larval arrest of *cth-2(mg599); moc-1(ok366)* mutant animals grown on MoaA *E. coli*. Transgenic *cth-2* expression by the native *cth-2*, the hypodermal, or the intestinal promoters displayed strong rescue activity (Fig. 6B). *cth-2* expressed in the muscle also displayed weak rescue activity while *cth-2* expressed in neurons did not rescue (Fig. 6B). These transgenes did not affect *cth-2; moc-1* double mutant worms when animals were



cultured on wild-type *E. coli*. These data suggest that CTH-2-mediated sulfur amino acid catabolism occurs in the *C. elegans* hypodermis, intestine, and muscle.

## Discussion

The ability to synthesize Moco is conserved across all kingdoms of life and organisms have previously been thought to rely solely upon *de novo* synthesis to maintain Moco homeostasis. Here show that *C. elegans* imports microbial Moco and the Moco precursor cPMP from the bacteria on which it feeds. The interkingdom transfer of these metabolites raises the possibility that transport of cPMP/Moco between cells, tissues, and organisms may be widespread. Ancient and nearly universal enzyme cofactors such as B vitamins, heme, and enzyme cofactors such as Moco, have probably been shared between organisms for billions of years. Organisms become reliant on exogenous sources of these cofactors, often via evolutionary loss of biosynthetic pathways. For example, *C. elegans* and some parasitic nematodes have lost heme biosynthetic enzymes, now acquiring heme solely from dietary sources<sup>21</sup>. The evolutionary maintenance or loss of cofactor biosynthesis and acquisition pathways is likely a function of bioavailability of the cofactor and the metabolic cost of producing the cofactor *de novo*. For *C. elegans*, it appears beneficial to have retained both the ability to synthesize Moco as well as to acquire it from its microbial diet.

In what state is Moco transferred from *E. coli* to *C. elegans*? There is no known pool of free or stored Moco in bacterial cells and the oxygen sensitivity of the mature cofactor make it unlikely that unbound Moco is the transferred molecule. It is possible that *C. elegans* ingests Moco bound to the bacterial Moco-utilizing proteins or the Moco-biosynthetic enzymes, and that this protein-cofactor interaction protects the cofactor during the uptake process. In this model, *C. elegans* would extract Moco from the *E. coli* proteins and incorporate it into its own Moco-requiring enzymes, such as SUOX-1. The mechanism of Moco transfer from bacteria to nematode remains to be discovered.

Could the inter-cellular transfer of cPMP and Moco be a conserved phenomenon? Cells from humans with Moco deficiency (MoCD) secrete the Moco-intermediate cPMP which can be acquired by cells *in vitro*<sup>22</sup>. This work laid the foundation for the idea of treating Moco deficiency with cPMP supplementation; 21 years later, a human MoCD patient was successfully treated with intravenous cPMP<sup>23</sup>. cPMP supplementation is only efficacious if patients possess the enzymes to convert cPMP into mature Moco. The successful treatment of human MoCD patients with cPMP parallels the ability of *C. elegans* to acquire cPMP from dietary *E. coli*, and suggest that this might be a conserved phenomenon. Furthermore, our demonstration of transfer of mature Moco from *E. coli* to *C. elegans* offers hope to deliver mature Moco, perhaps even from the microbiome, as a therapy to treat MoCD in patients that are refractory to cPMP treatment.

Why is Moco essential? In addition to its role as a cofactor, some Moco-biosynthetic enzymes have additional conserved activities such as tRNA thiolation (MOCS3) and promotion of glycine receptors clustering in neurons (Gephyrin)<sup>24–26</sup>. Our genetic suppressors of Moco-deficient larval arrest identified mutations in cystathionine gamma-lase (*cth-2*) or cysteine dioxygenase (*cdo-1*). These enzymes catalyze sequential steps in

the catabolism of methionine and cysteine. Our pharmacological studies demonstrate that sulfite produced by these enzymes is the key toxin that causes developmental arrest during Moco deficiency. While the exact mechanism by which sulfites are toxic to *C. elegans* is mysterious, sulfites are known to biochemically alter RNA, DNA, and proteins<sup>27–29</sup>. Sulfite also reacts with cystine to produce S-sulfocysteine (SSC), which is structurally similar to glutamate and a potent trigger of neural cell death<sup>30</sup>. Whether these modes of toxicity contribute to the inviability of Moco- and SUOX-1-deficient *C. elegans* is unknown. Humans are exposed to both endogenous sulfites, via catabolism of dietary methionine and cysteine<sup>6</sup>, and exogenous sulfites due to their widespread use as food preservatives<sup>27</sup>. These sulfites are detoxified by the Moco-requiring sulfite oxidase enzyme which oxidizes sulfite to sulfate to be excreted<sup>31,32</sup>. Our suppressor mutations in *cth-2* or *cdo-1* block the production of sulfites that accumulate during Moco deficiency, permitting growth and development. This is a conserved phenomenon: reducing sulfite production by limiting dietary intake of methionine and cysteine yields biochemical and clinical improvements in human patients with mild sulfite oxidase deficiency<sup>33,34</sup>. Thus, inhibition of cystathionine gamma-lyase or cysteine dioxygenase in human patients suffering from MoCD or sulfite oxidase deficiency might further alleviate the toxicity of endogenously produced sulfites.

Our tissue-specific rescue studies of *suox-1* suggest that the hypodermis is the major site of SUOX-1-mediated sulfite detoxification. We also found that the hypodermis is the major site of Moco biosynthesis (Fig. 6A). These data suggest that Moco is both synthesized (via MOC-1) and utilized (via SUOX-1) primarily in the hypodermis. However, the muscle is also a site of MOC-1-mediated Moco biosynthesis, but is not a site of SUOX-1 activity. A possible explanation for this asymmetry of Moco synthesis and utilization is that Moco may be synthesized in muscle and transported to the hypodermis where it supports SUOX-1 activity. Intestine-specific expression of *moc-1* does not rescue the *moc-1* inviability when animals are grown on Moco-deficient *E. coli*, suggesting that the intestine is not a site of Moco biosynthesis. Given that dietary *E. coli*-derived Moco can support the growth and development of *moc-1* mutant worms, these results suggest that dietary Moco is taken up through the intestine and transported to the hypodermis to support SUOX-1 activity. Therefore, the intestine may be specialized in uptake and distribution of dietary Moco while the muscle and hypodermis may be the primary sites of endogenous Moco synthesis. Identifying the mechanisms by which endogenous and dietary Moco are transported between animal tissues will be an exciting area of future research.

## Online Methods:

### Caenorhabditis elegans:

*C. elegans* strains were cultured at 20°C on nematode growth medium (NGM) seeded with *E. coli* OP50 unless otherwise noted<sup>35</sup>. The wild-type strain was Bristol N2. All *C. elegans* strains used in this work, their developmental stage at time of experiment, culture conditions, outcrossing status, and their sources are listed in Supplementary Table 3 or in the appropriate figure legend.

**Bacteria:**

The wild-type bacterial strains were *E. coli* (OP50) or *E. coli* (K-12) as indicated in the figure legends and Method Details section. All bacterial strains used in this work, their culture conditions, and their sources are listed in Supplementary Table 3 or the appropriate figure legends.

**Plasmid construction and transgenesis:**

All plasmids utilized in this manuscript are listed in Supplementary Table 3. All cloning was performed using isothermal/Gibson assembly in a pBluescript plasmid backbone<sup>36</sup>. Tissue-specific rescue plasmids were constructed by amplifying the *suox-1*, *moc-1*, and *cth-2* genomic loci from wild-type *C. elegans* genomic DNA. Each locus was amplified from the start codon to the stop codon including all exons and introns and inserted into plasmids that contained the appropriate tissue specific promoter and C-terminal green fluorescent protein. For these plasmids, the stop codon was mutated to allow translation of C-terminal GFP. For *Pmoc-1::MOC-1::GFP* (pKW26) and *Pcth-2::CTH-2::GFP* (pKW23) the entire genomic locus including upstream promoter, 5'UTR, exons, and introns were amplified in a single polymerase chain reaction and inserted into plasmids that contained C-terminal GFP. The *moc-1* promoter was the 874bp upstream of the *moc-1* start codon. The *cth-2* promoter was the 3,965bp of the *cth-2* start codon. The tissue-specific promoters used in this work are *rpl-28* (all tissues), *sng-1* (neurons), *vha-6* (intestine), *myo-3* (muscle), and *col-10* (hypodermis). The *rpl-28* promoter was the 605bp upstream of the *rpl-28* start codon. The *sng-1* promoter used was the 2,080bp upstream of the *sng-1* start codon. The *vha-6* promoter used was the 934bp upstream of the *vha-6* start codon. The *myo-3* promoter was the 2,168bp upstream of the *myo-3* start codon. The *col-10* promoter was the 1,129bp upstream of the *col-10* start codon. For information on the cloning of *Pmoc-5::MOC-5* (pKW20) see "Identification of F49E2.1/*moc-5* and W01A11.6/*moc-2* as genes required for growth during dietary Moco deficiency."

Transgenic animals containing extrachromosomal arrays were generated by injecting the gonad of worms with a plasmid of interest and a co-injection marker<sup>37</sup>. The co-injection marker was *Pmyo-2::mCherry* for all strains analyzed in this manuscript except for GR2258 which utilized a *Pmyo-3::GFP* co-injection marker<sup>38</sup>. All transgenic *C. elegans* strains are listed in Supplementary Table 3.

***C. elegans* growth assays:**

*C. elegans* were synchronized at the first stage of larval development (L1). L1 animals were then cultured on NGM seeded with wild-type or mutant *E. coli* K-12. The strains of *E. coli* used are noted specifically for each assay and are listed in Supplementary Table 3.

For cysteine, sulfite, or sulfate sensitivity assays, NGM was seeded with wild-type or MoaA *E. coli* K-12 and then supplemented with various concentrations of L-cysteine (0, 0.00062, 0.0012, 0.0031, 0.0062, and 0.12M), sodium metabisulfite (0.005M), or sodium sulfate (0.005M). Synchronized L1 animals were placed onto the various cysteine, sulfite, or sulfate culture conditions and were allowed to develop for 48 or 72 hours (specified in figure legends) at 20°C.

For all assays, after the growth period was completed live animals were imaged using an Axio Zoom.V16 microscope (Zeiss) equipped with an ORCA-Flash4.0 digital camera (Hamamatsu). Images were captured using ZEN software (Zeiss) and processed utilizing ImageJ. Animal length was measured from the tip of the head to the end of the tail. The concentration of supplemental cysteine that caused 50% of the wild-type growth (IC50) was calculated with nonlinear regression analyses using GraphPad Prism software.

#### **Quantification of embryo hatching rate:**

To determine the hatching rate of wild-type and mutant *C. elegans* when cultured under various growth conditions, we performed synchronized egg lays using young adults. Embryos were then scored for hatching 12–24 hours after being laid. To facilitate adult-specific Moco deficiency, in some experiments L4 animals were shifted onto either wild-type or MocoA *E. coli*, allowed to develop to the young adult stage and their progeny were assayed for their ability to hatch. All experiments were performed at 20°C unless otherwise noted.

#### **Screening for *E. coli* gene activities required for the growth and development of *C. elegans* lacking endogenous Moco biosynthesis:**

To identify *E. coli* gene activities that are required for the growth of *moc-1(ok366)* animals, we utilized the Keio collection of deletion *E. coli* strains (NIG). Each of the approximately 4,000 deletion strains are derived from the *E. coli* K-12 strain BW25113<sup>12</sup>. Each strain was cultured overnight in LB with 50 µg/ml kanamycin. 0.1ml of this 2ml overnight culture was seeded on NGM and allowed to dry and grow overnight at room temperature (~22–23°C) creating a lawn of bacteria.

Concurrently, approximately 200,000 *moc-1(ok366)* animals grown on *E. coli* OP50, which is wild type for Moco biosynthetic pathway genes, were prepared with sodium hypochlorite to generate eggs and sterilize the *E. coli* from the parental feeding. These eggs were then allowed to hatch overnight without food and were synchronized at the L1 stage. 30–50 L1 animals were dispersed onto each unique deletion strain of *E. coli*. These animals were cultured for 2 days at room temperature (~22–23°C). Wells were then scored for growth. Here we report deletion strains of *E. coli* that caused early larval growth arrest of *moc-1(ok366)* animals.

To more cleanly analyze the *E. coli* strains identified in our screen, we used established methods to remove the kanamycin resistance cassette from each Keio strain of interest<sup>12</sup>. This process results in the deletion of the *E. coli* gene of interest and leaves behind a sequence that codes for a 34 amino acid peptide. Importantly, this peptide coding sequence is in frame, allowing downstream genes in that operon to be functional. Thus, these deletions are nonpolar and allowed genetic interpretation of the single gene knockout. Nonpolar mutant strains were utilized in Figure 1C,D, Figure 2, and Supplementary Figure 3. All other strains still contained the kanamycin resistance cassette and might be polar, thus affecting the entire operon of interest.

### Identification of F49E2.1/*moc-5* and W01A11.6/*moc-2* as genes required for growth during dietary Moco deficiency:

To define *C. elegans* gene activities that were required for growth during dietary Moco deficiency, we carried out a chemical mutagenesis screen for animals that were unable to grow and develop on MoaA *E. coli*. Wild-type *C. elegans* were mutagenized with ethyl methanesulfonate (EMS) and grown on wild-type *E. coli* for two generations. We then screened for mutant animals in the F2 generation that failed to develop when cultured on MoaA *E. coli* but grew well on wild-type *E. coli*<sup>35</sup>. We isolated two mutant alleles in this screen, *mg589* and *mg639*.

Using whole genome sequencing and linkage analyses we determined that *mg589* was located on the X linkage group (LG) and identified 5 candidate lesions on LG X that might be the *mg589* mutation. Candidate lesions were homozygous and were predicted to alter the protein sequence. One of these 5 candidates, F49E2.1, is homologous to *E. coli* MoaA and MoaC, genes with established roles in Moco biosynthesis. F49E2.1 has a long isoform F49E2.1b and a short isoform F49E2.1a, both of which are predicted to use the same start codon. The lesion in F49E2.1 changes a Gga glycine codon to an Aga encoding an arginine. This missense mutation results in a G303R change in the encoded peptide. Interestingly, glycine 303 is conserved in *E. coli* MoaA, *C. elegans* F49E2.1, and human MOCS1 suggesting its functional importance. Glycine 303 is present in both isoforms of F49E2.1.

Our linkage, sequencing, and homology data strongly suggested F49E2.1 was the gene affected by *mg589*. To independently demonstrate this, we rescued *mg589* mutant animals with the F49E2.1 wild-type genomic locus. To generate the rescuing plasmid, we engineered pBluescript to contain the entire wild-type F49E2.1 locus from 1,502 base pairs upstream of the ATG start codon to 722 base pairs downstream of the F49E2.1b stop codon. Thus, the rescuing plasmid (pKW20, F49E2.1(+), also known as *Pmoc-5::MOC-5*) contained the endogenous promoter, exons, introns and untranslated regions of both F49E2.1a and F49E2.1b and no other genes.

Transgenic animals containing extrachromosomal arrays were generated by injecting the gonad of *mg589* mutant worms with pKW20 and a *Pmyo-3::GFP* co-injection marker<sup>37,38</sup>. *Pmyo-3::GFP* is a plasmid with the *myo-3* promoter driving the expression of green fluorescent protein (GFP) in the body wall muscles. Transgenic strains were selected and maintained based on the heritable transmission of GFP in the body wall muscle. We isolated 4 independently derived transgenic *mg589* strains expressing F49E2.1(+).

To test the ability of F49E2.1 to rescue the *mg589* phenotype, we cultured *mg589* + F49E2.1(+) animals and their nontransgenic siblings on MoaA *E. coli*. For all 4 transgenic strains isolated, the transgenic *mg589* + F49E2.1(+) animals grew and developed well on MoaA *E. coli* while the nontransgenic sibling *mg589* animals did not. These results demonstrate that the F49E2.1 genetic locus rescued the *mg589* growth defect during dietary Moco deficiency. Thus, based on linkage, sequencing, homology, and rescue data, we conclude that F49E2.1 is the gene affected by the *mg589* mutation. We rename F49E2.1 as *moc-5* for molybdenum cofactor biosynthesis.

Using whole genome sequencing and linkage analyses we determined that *mg639* was located on LG V and identified 8 candidate lesions on LG V that might be the *mg639* mutation. Candidate lesions were homozygous and were predicted to alter the protein sequence. One of these 8 candidates, *moc-2*, is homologous to *E. coli* MogaA, a gene with an established role in Moco biosynthesis. The lesion in *moc-2* changes a gCa alanine codon to a gTa encoding a valine. This missense mutation results in an A136V change in the encoded peptide.

Our linkage, sequencing, and homology data strongly suggested *moc-2* was the gene affected by *mg639*. However, the sensitivity of animals carrying the *mg639* mutation to growth on MoaA *E. coli* was not as dramatic as other mutations in *C. elegans* Moco biosynthetic enzymes (Supplementary Fig. 6, Supplementary Table 2). Furthermore, A136V is likely to be a subtle loss-of-function as alanine and valine are very similar amino acids. Thus we speculated that *mg639* might be a hypomorphic allele of *moc-2*. To test this hypothesis and independently demonstrate that *moc-2* was the gene affected by *mg639*, we generated a presumptive null mutation in *moc-2* using CRISPR/Cas9 technology<sup>9</sup>. This allele results in a Gly72Stop followed by a frameshift to completely alter the codons downstream of the new mutant stop codon. The newly isolated mutation was designated *moc-2(mg595)*. *moc-2(mg595)* animals displayed complete larval arrest when cultured on MoaA *E. coli* (Fig. 2E). This independently isolated mutation phenocopies *moc-2(mg639)* and displays a more severe growth defect on MoaA *E. coli*. Thus, based on linkage, sequencing, homology, and phenocopy with an independent allele, we concluded that *moc-2* is the gene affected by the *mg639* mutation. Furthermore, we believe that *mg639* is a hypomorphic allele of *moc-2* while the newly generated *mg595* is likely a null allele. *mg595* is our reference allele for *moc-2* and was used for all the work in this manuscript unless otherwise noted.

### **EMS-mutagenesis screens for suppressors of *moc-2*, *moc-3*, and *moc-4* mutant growth arrest during Moco deficiency:**

To define *C. elegans* gene activities that mediate the growth arrest of *C. elegans* *moc* mutants fed on Moco-deficient *E. coli*, we carried out a chemical mutagenesis screen for suppressors of *C. elegans* *moc-2(mg595)*, *moc-3(ku300)*, or *moc-4(ok2571)* strains grown on Moco mutant *E. coli*. *moc-2(mg595)*, *moc-3(ku300)*, and *moc-4(ok2571)* *C. elegans* were mutagenized with ethyl methanesulfonate (EMS) and grown for two generations on wild-type *E. coli*. F2 animals were then synchronized as L1s, and challenged to grow and develop on MoaA *E. coli*. We screened >100,000 F1 genomes and isolated mutations that suppressed this larval arrest/lethality.

### **Identification of EMS-induced mutations via whole-genome sequencing and linkage analyses:**

The methods we used to identify EMS-induced mutations via whole-genome sequencing have been previously described<sup>18</sup>. Briefly, whole-genome DNA was prepared from *C. elegans* utilizing the Genra Puregene Tissue Kit (Qiagen) per the manufacturer's instructions. Genomic DNA libraries were prepared utilizing the NEBNext genomic DNA

library construction kit (New England Biolabs). DNA libraries were sequenced on an Illumina HiSeq instrument and deep sequencing reads were analyzed using CloudMap<sup>39</sup>.

We performed linkage analyses by mating a mutant strain of interest with the unmutagenized parental strain. Linkage analysis of *mg589* and *mg639* was performed by mating wild-type males with *mg589* or *mg639* hermaphrodites. Linkage analysis was also performed for a number of the *moc-3(ku300)* suppressors and was performed by mating *moc-3(ku300)* males with *moc-3(ku300);mg588* hermaphrodites (for example). The subset of *moc-3(ku300)* suppressors for which linkage analysis was performed is displayed in Supplementary Table 4. For each individual case, 20–50 F2 progeny of the linkage cross were collected that displayed the mutant phenotype. Each isolate represented a unique homozygous mutant strain that carried a unique set of recombination events. For each linkage cross, all F2 homozygous mutant animals were pooled and DNA was extracted. In downstream analyses, only EMS mutations that were tightly linked to the causative lesion remained homozygous, shrinking the candidate pool of causative lesions. The genes affected by mutations that were not analyzed using linkage analyses were identified because multiple alleles affected the same genes (i.e. *cth-2* and *cdo-1*). We noticed that no *cdo-1* mutations emerged from the screens to suppress *moc-3(ku300)* growth arrest on Moco-deficient *E. coli*. To ensure that *cdo-1* mutations do not specifically suppress *moc-2* and *moc-4* mutant *C. elegans*, we constructed the *moc-3(ku300);cdo-1(mg622)* double mutant and attempted to culture the strain on Moco-deficient *E. coli*. As expected, *cdo-1* loss of function also suppressed *moc-3* mutant growth arrest on Moco-deficient *E. coli* (Supplementary Fig. 7).

#### Analysis of *suox-1* null mutant:

The *suox-1(mg663)* allele is a 653 base pair deletion generated using CRISPR/Cas9 technology<sup>9</sup>. This mutation causes larval lethality and was balanced using the X balancer *tmC24*<sup>40</sup>.

#### Supplementary Material

Refer to Web version on PubMed Central for supplementary material.

#### Acknowledgements:

We thank the *Caenorhabditis* Genetics Center, Min Han, Victor Ambros, and Shohei Mitani for providing *C. elegans* strains. We thank Marie-Ann Félix for providing wild bacterial isolates and the National BioResource Project (NIG, Japan) for providing the Keio *E. coli* knockout collection. This work was funded by an NIH Grant (5R01GM044619–26) to G.R. and a Damon Runyon Fellowship (DRG-2293–16) to K.W.

#### References:

1. Schwarz G, Mendel RR & Ribbe MW Molybdenum cofactors, enzymes and pathways. *Nature* 460, 839–847 (2009). [PubMed: 19675644]
2. Zhang Y & Gladyshev VN Molybdoproteomes and Evolution of Molybdenum Utilization. *Journal of Molecular Biology* 379, 881–899 (2008). [PubMed: 18485362]
3. MacGregor CH Synthesis of nitrate reductase components in chlorate-resistant mutants of *Escherichia coli*. *J. Bacteriol* 121, 1117–1121 (1975). [PubMed: 1090592]
4. Reiss J & Hahnewald R Molybdenum cofactor deficiency: Mutations in GPHN, MOCS1, and MOCS2. *Hum. Mutat* 32, 10–18 (2010).

5. Huijmans JGM et al. Molybdenum cofactor deficiency: Identification of a patient with homozygote mutation in the MOCS3 gene. *Am. J. Med. Genet* 173, 1601–1606 (2017). [PubMed: 28544736]
6. Stipanuk MH SULFUR AMINO ACID METABOLISM: Pathways for Production and Removal of Homocysteine and Cysteine. *Annu. Rev. Nutr* 24, 539–577 (2004). [PubMed: 15189131]
7. Pepper ASR et al. The *C. elegans* heterochronic gene *lin-46* affects developmental timing at two larval stages and encodes a relative of the scaffolding protein gephyrin. *Development* 131, 2049–2059 (2004). [PubMed: 15073154]
8. Kim S et al. Allele-specific suppressors of *lin-1*(R175Opal) identify functions of MOC-3 and DPH-3 in tRNA modification complexes in *Caenorhabditis elegans*. *Genetics* 185, 1235–1247 (2010). [PubMed: 20479142]
9. Arribere JA et al. Efficient marker-free recovery of custom genetic modifications with CRISPR/Cas9 in *Caenorhabditis elegans*. *Genetics* 198, 837–846 (2014). [PubMed: 25161212]
10. Samuel BS, Rowedder H, Braendle C, Félix M-A & Ruvkun G *Caenorhabditis elegans* responses to bacteria from its natural habitats. *Proc. Natl. Acad. Sci. U.S.A* 113, E3941–9 (2016). [PubMed: 27317746]
11. Dirksen P et al. The native microbiome of the nematode *Caenorhabditis elegans*: gateway to a new host-microbiome model. *BMC Biol.* 14, 38 (2016). [PubMed: 27160191]
12. Baba T et al. Construction of *Escherichia coli* K-12 in-frame, single-gene knockout mutants: the Keio collection. *Mol Syst Biol* 2, 1–11 (2006).
13. Self WT, Grunden AM, Hasona A & Shanmugam KT Molybdate transport. *Res. Microbiol* 152, 311–321 (2001). [PubMed: 11421278]
14. Datsenko KA & Wanner BL One-step inactivation of chromosomal genes in *Escherichia coli* K-12 using PCR products. *Proc. Natl. Acad. Sci. U.S.A* 97, 6640–6645 (2000). [PubMed: 10829079]
15. Wuebbens MM & Rajagopalan KV Investigation of the Early Steps of Molybdopterin Biosynthesis in *Escherichia coli* through the Use of in Vivo Labeling Studies. *J. Biol. Chem* 270, 1082–1087 (1995). [PubMed: 7836363]
16. Reschke S et al. Identification of a bis-molybdopterin intermediate in molybdenum cofactor biosynthesis in *Escherichia coli*. *J. Biol. Chem* 288, 29736–29745 (2013). [PubMed: 24003231]
17. Rosentel JK, Healy F, Maupin-Furlow JA, Lee JH & Shanmugam KT Molybdate and regulation of *mod* (molybdate transport), *fdhF*, and *hyc* (formate hydrogenylase) operons in *Escherichia coli*. *J. Bacteriol* 177, 4857–4864 (1995). [PubMed: 7665461]
18. Lehrbach NJ, Ji F & Sadreyev R Next-Generation Sequencing for Identification of EMS-Induced Mutations in *Caenorhabditis elegans*. *Curr Protoc Mol Biol* 117, 7.29.1–7.29.12 (2017). [PubMed: 28060408]
19. Oshino N & Chance B The properties of sulfite oxidation in perfused rat liver; interaction of sulfite oxidase with the mitochondrial respiratory chain. *Archives of Biochemistry and Biophysics* 170, 514–528 (1975). [PubMed: 1190778]
20. Thompson O et al. The million mutation project: a new approach to genetics in *Caenorhabditis elegans*. *Genome Research* 23, 1749–1762 (2013). [PubMed: 23800452]
21. Rao AU, Carta LK, Lesuisse E & Hamza I Lack of heme synthesis in a free-living eukaryote. *Proc. Natl. Acad. Sci. U.S.A* 102, 4270–4275 (2005). [PubMed: 15767563]
22. Johnson JL, Wuebbens MM, Mandell R & Shih VE Molybdenum cofactor biosynthesis in humans. Identification of two complementation groups of cofactor-deficient patients and preliminary characterization of a diffusible molybdopterin precursor. *J. Clin. Invest* 83, 897–903 (1989). [PubMed: 2522104]
23. Veldman A et al. Successful Treatment of Molybdenum Cofactor Deficiency Type A With cPMP. *PEDIATRICS* 125, e1249–e1254 (2010). [PubMed: 20385644]
24. Leimkühler S Shared function and moonlighting proteins in molybdenum cofactor biosynthesis. *Biol. Chem* 398, 1009–1026 (2017). [PubMed: 28284029]
25. Chowdhury MM, Dosche C, Löhmannsröben H-G & Leimkühler S Dual role of the molybdenum cofactor biosynthesis protein MOCS3 in tRNA thiolation and molybdenum cofactor biosynthesis in humans. *J. Biol. Chem* 287, 17297–17307 (2012). [PubMed: 22453920]
26. Kirsch J, Wolters I, Triller A & Betz H Gephyrin antisense oligonucleotides prevent glycine receptor clustering in spinal neurons. *Nature* 366, 745–748 (1993). [PubMed: 8264797]



27. Gunnison AF Sulphite toxicity: a critical review of in vitro and in vivo data. *Food Cosmet Toxicol* 19, 667–682 (1981). [PubMed: 6171492]
28. Bailey JL & Cole RD Studies on the reaction of sulfite with proteins. *J. Biol. Chem* 234, 1733–1739 (1959). [PubMed: 13672955]
29. Würfel M, Häberlein I & Follmann H Inactivation of thioredoxin by sulfite ions. *FEBS Lett* 268, 146–148 (1990). [PubMed: 2200707]
30. Kumar A et al. S-sulfocysteine/NMDA receptor-dependent signaling underlies neurodegeneration in molybdenum cofactor deficiency. *J. Clin. Invest* 127, 4365–4378 (2017). [PubMed: 29106383]
31. Mårtensson J The effects of short-term fasting on the excretion of sulfur compounds in healthy subjects. *Metab. Clin. Exp* 31, 487–492 (1982). [PubMed: 7078429]
32. Wattiaux-de Coninck S & Wattiaux R Subcellular distribution of sulfite cytochrome c reductase in rat liver tissue. *Eur. J. Biochem* 19, 552–556 (1971). [PubMed: 4325350]
33. Touati G et al. Dietary therapy in two patients with a mild form of sulphite oxidase deficiency. Evidence for clinical and biological improvement. *J. Inherit. Metab. Dis* 23, 45–53 (2000). [PubMed: 10682307]
34. Del Rizzo M et al. Metabolic stroke in a late-onset form of isolated sulfite oxidase deficiency. *Mol. Genet. Metab* 108, 263–266 (2013). [PubMed: 23414711]

### Methods-only References:

35. Brenner S The genetics of *Caenorhabditis elegans*. *Genetics* 77, 71–94 (1974). [PubMed: 4366476]
36. Gibson DG et al. Enzymatic assembly of DNA molecules up to several hundred kilobases. *Nat. Methods* 6, 343–345 (2009). [PubMed: 19363495]
37. Mello CC, Kramer JM, Stinchcomb D & Ambros V Efficient gene transfer in *C.elegans*: extrachromosomal maintenance and integration of transforming sequences. *EMBO J* 10, 3959–3970 (1991). [PubMed: 1935914]
38. Frøkjær-Jensen C et al. Single-copy insertion of transgenes in *Caenorhabditis elegans*. *Nat. Genet* 40, 1375–1383 (2008). [PubMed: 18953339]
39. Minevich G, Park DS, Blankenberg D, Poole RJ & Hobert O CloudMap: a cloud-based pipeline for analysis of mutant genome sequences. *Genetics* 192, 1249–1269 (2012). [PubMed: 23051646]
40. Dejima K et al. An Aneuploidy-Free and Structurally Defined Balancer Chromosome Toolkit for *Caenorhabditis elegans*. *Cell Rep* 22, 232–241 (2018). [PubMed: 29298424]

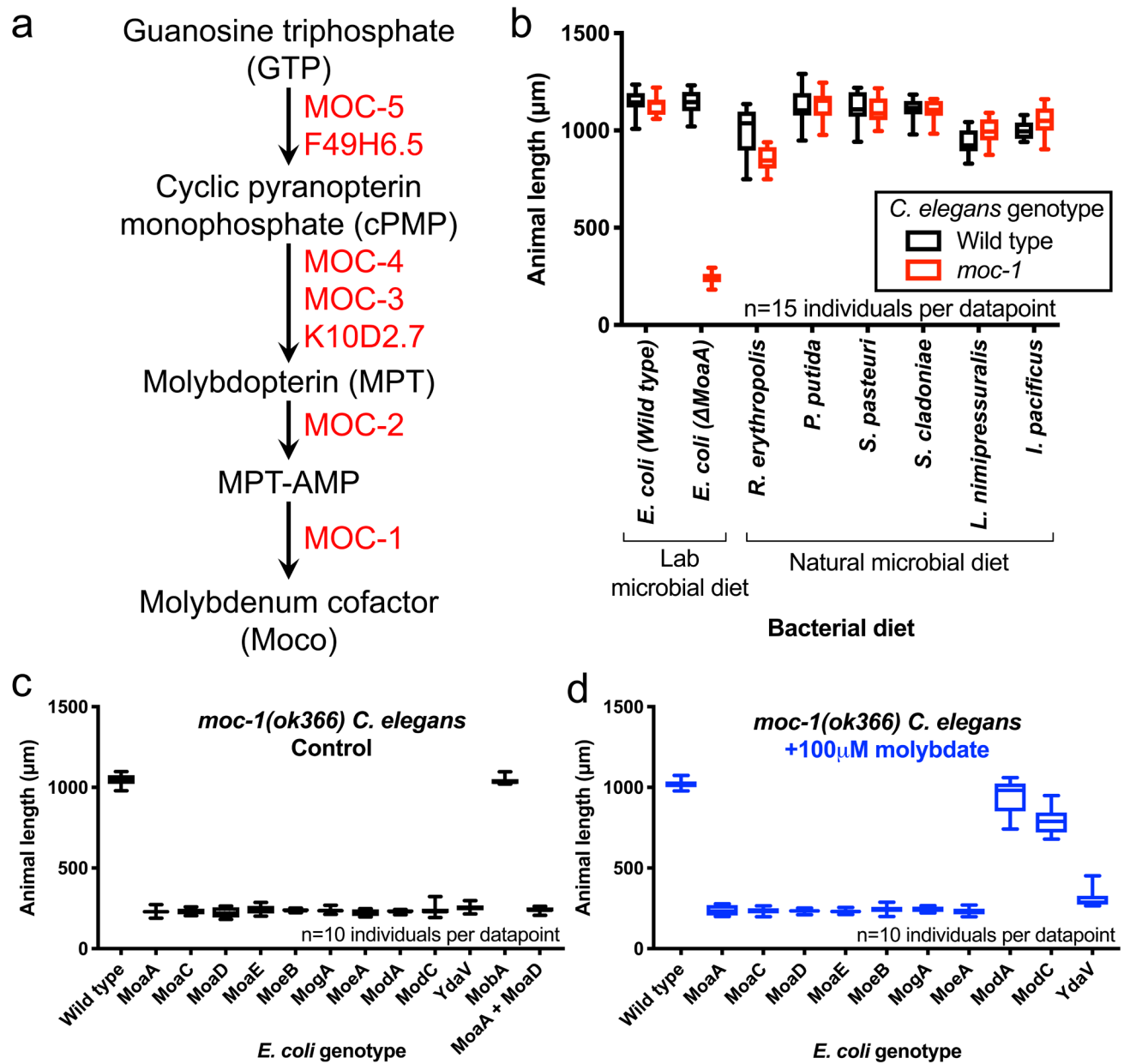


**Figure 1: Moco acquisition and biosynthesis are redundantly required for life in *C. elegans*.** (A) By protein sequence homology to human and bacterial Moco biosynthetic enzymes, the inferred *C. elegans* Moco biosynthesis pathway is displayed. (B) The growth of wild-type and *moc-1(ok366)* animals on either wild-type or *MoaA E. coli* (lab microbial diet) or 6 bacterial strains native to the *Caenorhabditis* ecosystem (natural microbial diet) was quantified after 72 hours of growth from the first larval stage. (C,D) The growth of *moc-1(ok366)* animals on either wild-type or mutant *E. coli* was quantified after 72 hours of growth from the first larval stage. Before being fed to *C. elegans*, the wild-type and mutant *E. coli* strains were initially cultured without (C, Control) or with 100 $\mu\text{M}$  sodium molybdate (D, +100 $\mu\text{M}$  molybdate) in LB. The mutant *E. coli* strains used here are nonpolar deletions

of the indicated genes, except for the MobA mutant strain which still has the Kanamycin resistance cassette inserted into the MobA open reading frame<sup>12</sup>. Box plots display the median, upper, and lower quartiles while whiskers indicate minimum and maximum data points. Sample size (n) is displayed for each experiment.

Author Manuscript

Author Manuscript

Author Manuscript

Author Manuscript

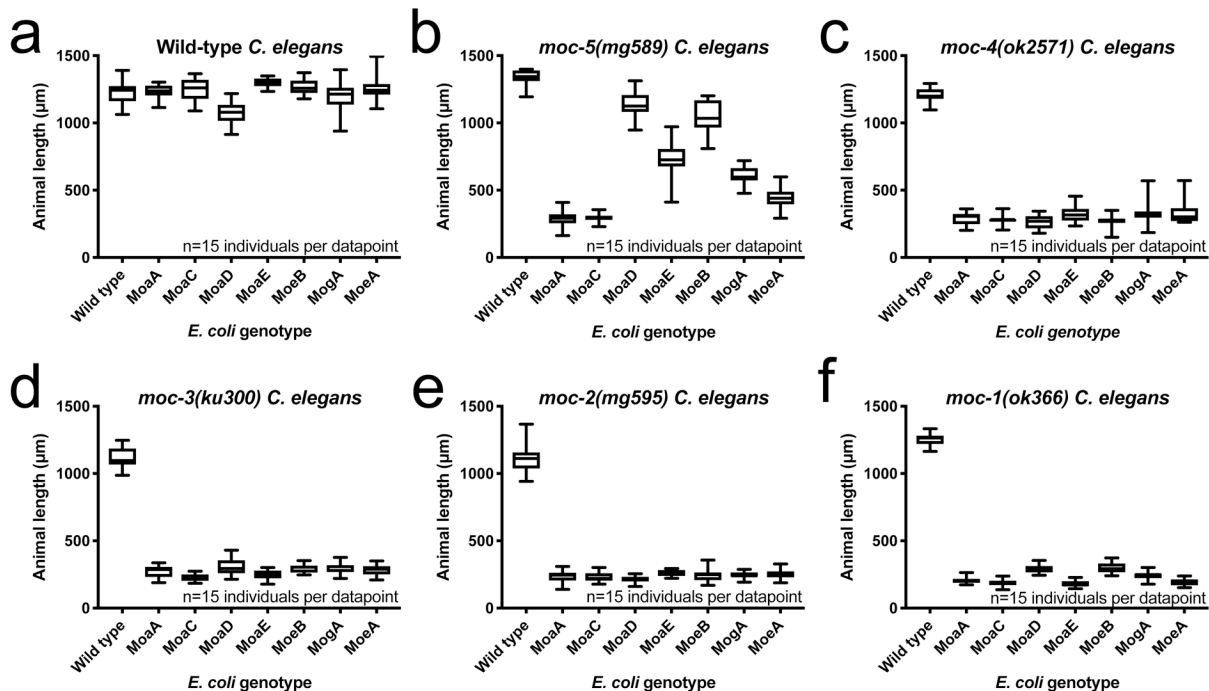


**Figure 2: *C. elegans* acquire cPMP and Moco from dietary *E. coli*.**

(A) Wild-type, (B) *moc-5(mg589)*, (C) *moc-4(ok2571)*, (D) *moc-3(ku300)*, (E) *moc-2(mg595)*, and (F) *moc-1(ok366)* animals were cultured from synchronized L1 larvae for 72 hours on wild-type and mutant *E. coli* disrupted at distinct steps in Moco biosynthesis. *E. coli* mutations used here are nonpolar and should not disrupt other genes in their operons. Animal lengths were determined for each condition. The *moc-1(ok366)* mutation is a 1.4kb deletion that is predicted to be a null allele. The *moc-4(ok2571)* mutation is a 1.8kb deletion that is predicted to be a null allele. *moc-2(mg595)* encodes a (Gly72Stop) followed by a frameshift that is likely a null allele. *moc-3(ku300)* is an established genetic reagents that represents a likely loss-of-function or null allele<sup>8</sup>. *moc-5(mg589)* is a missense mutation (G303R) substitution loss-of-function or null allele. Box plots display the median, upper, and lower quartiles while whiskers indicate minimum and maximum data points. Sample size (n) is displayed for each experiment.

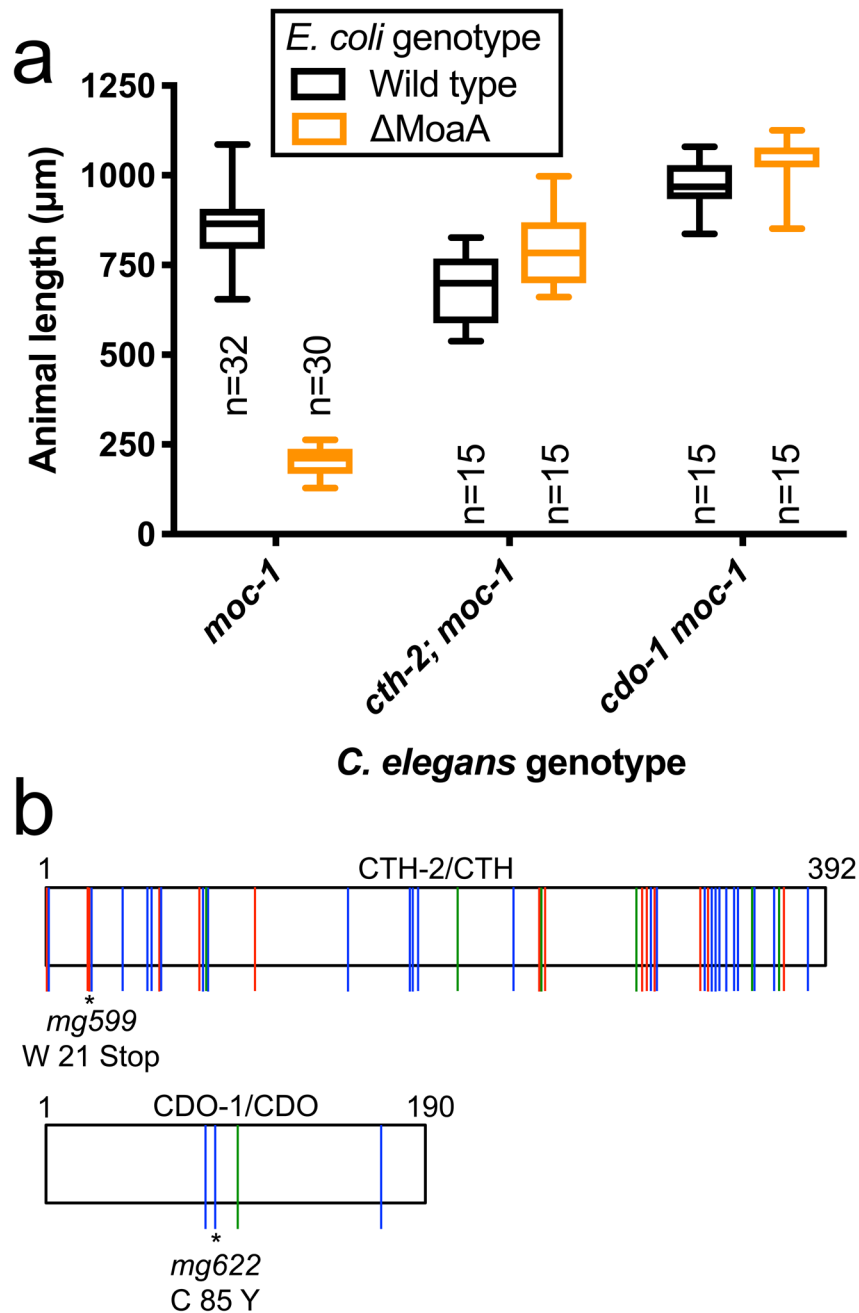


**Figure 3: *cth-2* and *cdo-1* are necessary for the growth arrest and death caused by Moco deficiency.**

(A) *moc-1(ok366)*, *cth-2(mg599);moc-1(ok366)*, and *cdo-1(mg622) moc-1(ok366)* mutant animals were synchronized at the L1 stage and cultured on wild-type and  $\Delta\text{MoaA}$  *E. coli* for approximately 48 hours. Animal lengths were determined for each condition. Box plots display the median, upper, and lower quartiles while whiskers indicate minimum and maximum data points. Sample size (n) is the number of individuals assayed and is displayed for each experiment. (B) Cartoons of CTH-2 (upper) and CDO-1 (lower) proteins. Colored vertical lines indicate amino acid substitutions identified in our screen as suppressors of

(green) *moc-2(mg595)*, (red) *moc-3(ku300)*, or (blue) *moc-4(ok2571)* mutant *C. elegans* when cultured on MoeA *E. coli*. \*, reference alleles for each gene.

Author Manuscript

Author Manuscript

Author Manuscript

Author Manuscript

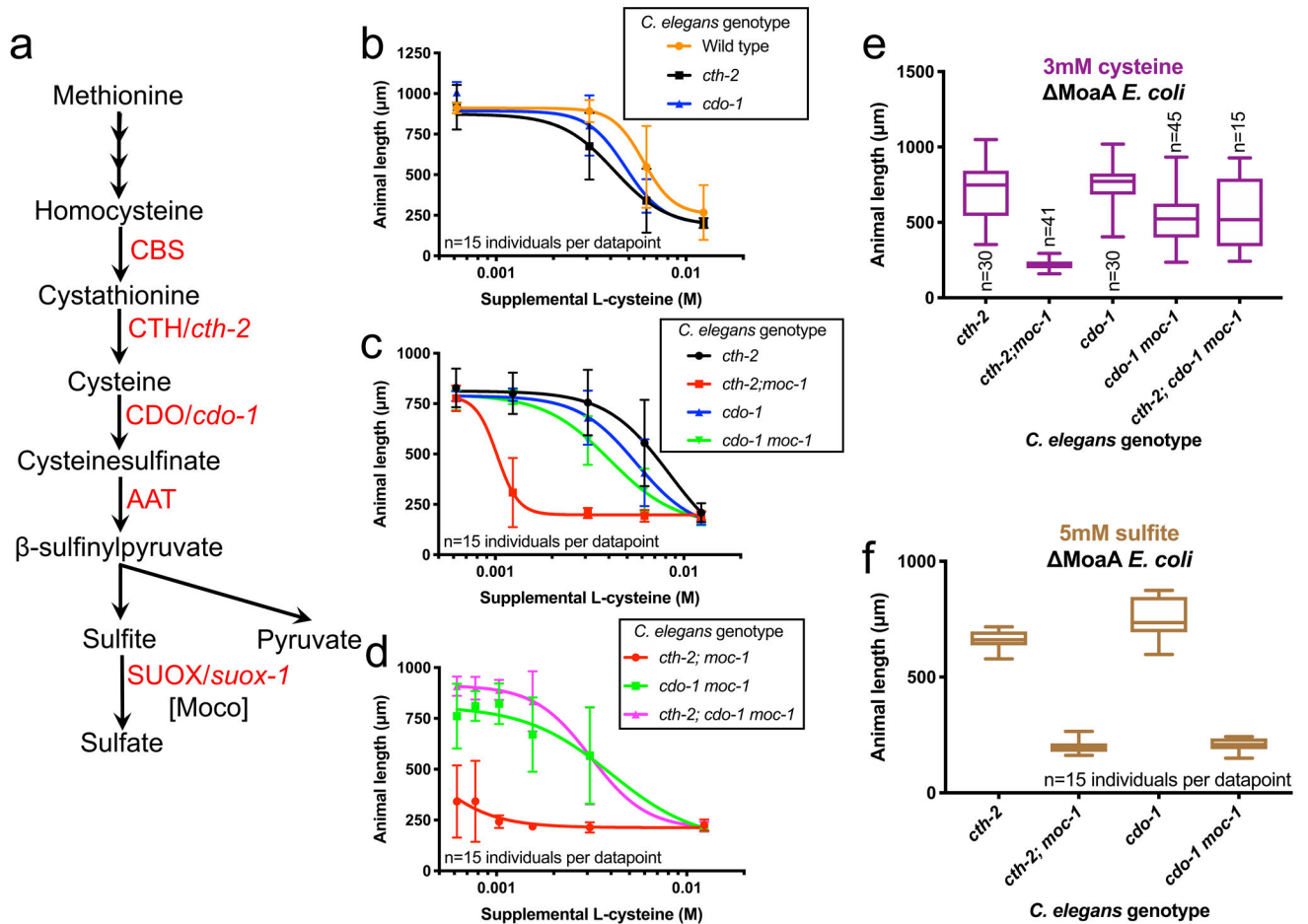


**Figure 4: Endogenously produced sulfites inhibit growth and development during Moco deficiency.**

(A) Simplified cartoon of sulfur amino acid catabolism beginning with methionine. Here we highlight the roles of CTH/*cth-2*, CDO/*cdo-1*, and the Moco requiring enzyme SUOX/*suox-1*. CBS is cystathionine beta synthase and AAT is aspartate aminotransferase. (B-F) Wild-type, *cth-2*(*mg599*), *cdo-1*(*mg622*), *cth-2*(*mg599*);*moc-1*(*ok366*), *cdo-1*(*mg622*) *moc-1*(*ok366*) and *cth-2*(*mg599*); *cdo-1*(*mg622*) *moc-1*(*ok366*) animals were cultured from the first larval stage on MoaA *E. coli* supplemented with various concentrations of (B-E) cysteine or (F) 5mM sulfite. Animals were cultured for 48 hours and animal lengths were quantified. (B-D) Average values and standard deviation are displayed for each concentration of supplemental cysteine. (E,F) Growth of *C. elegans* mutants was scored on (E) 3mM supplemental cysteine or (F) 5mM supplemental sulfite. Box plots display the median, upper, and lower quartiles while whiskers indicate minimum and maximum data points. Sample size (n) is the number of individuals assayed and is displayed for each experiment. The data in Figure 4E summarizes the data in Figures 4B–D, highlighting the critical 3mM concentration of supplemental cysteine.

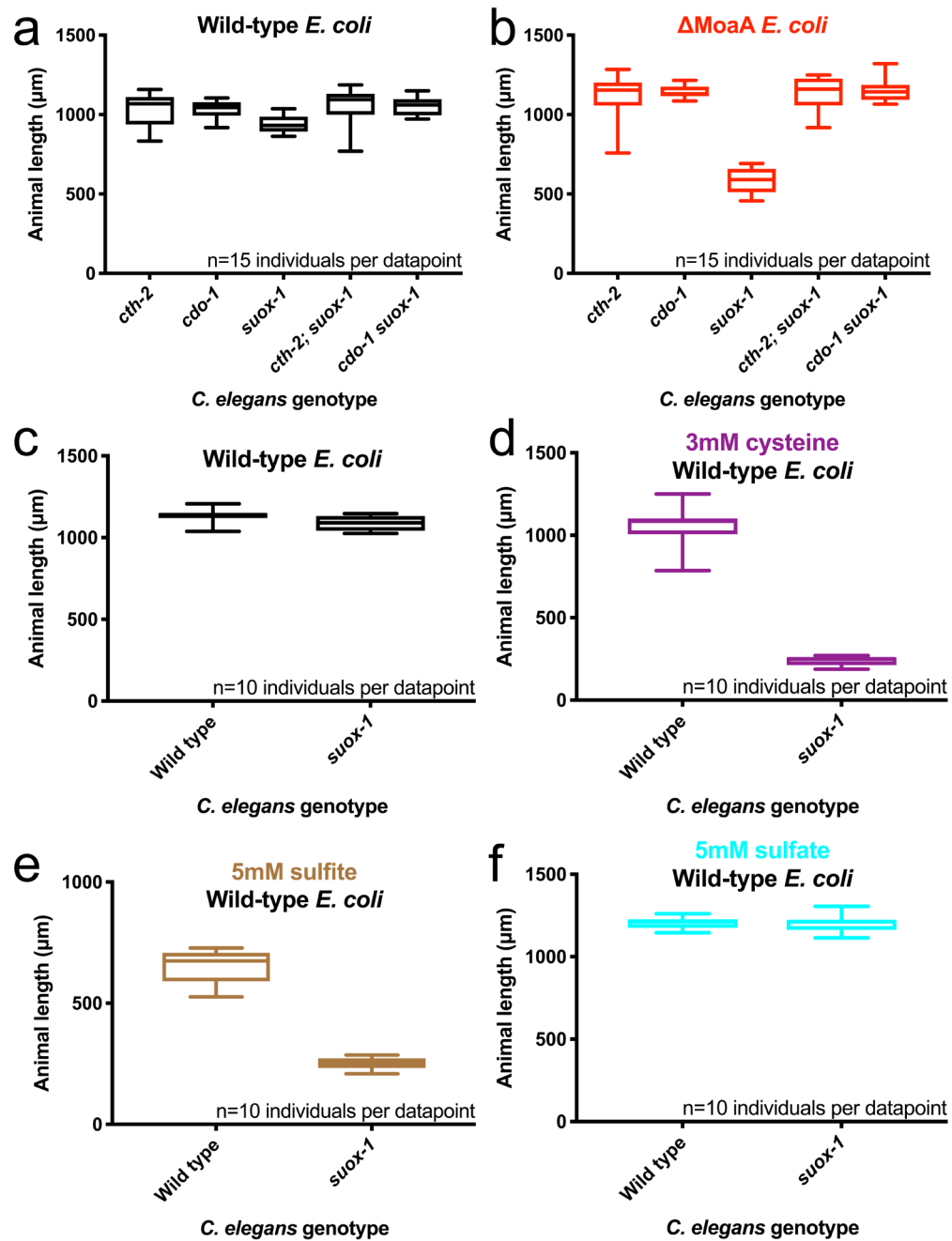


**Figure 5: *suox-1* hypomorphic allele phenocopies Moco deficiency in *C. elegans*.**

Analyses of the *suox-1*(*gk738847*) hypomorphic allele: *cth-2*(*mg599*), *cdo-1*(*mg622*), *suox-1*(*gk738847*), *cth-2*(*mg599*);*suox-1*(*gk738847*), and *cdo-1*(*mg622*) *suox-1*(*gk738847*) animals were cultured from the first larval stage on (A) wild-type or (B) MoaA *E. coli*. (C-F) Wild-type or *suox-1*(*gk738847*) mutant animals were cultured from the first larval stage on (C) wild-type *E. coli*, or wild-type *E. coli* supplemented with (D) 3mM cysteine, (E) 5mM sulfite, or (F) 5mM sulfate. Animals were cultured for 72 hours and animal lengths were quantified. Box plots display the median, upper, and lower quartiles while whiskers indicate minimum and maximum data points. Sample size (n) is displayed for each



experiment. Please note, the wild-type data points displayed in Figure 5C–F are also displayed in Supplementary Fig.5, as these assays were performed in parallel and utilize the same wild-type controls.

Author Manuscript

Author Manuscript

Author Manuscript

Author Manuscript

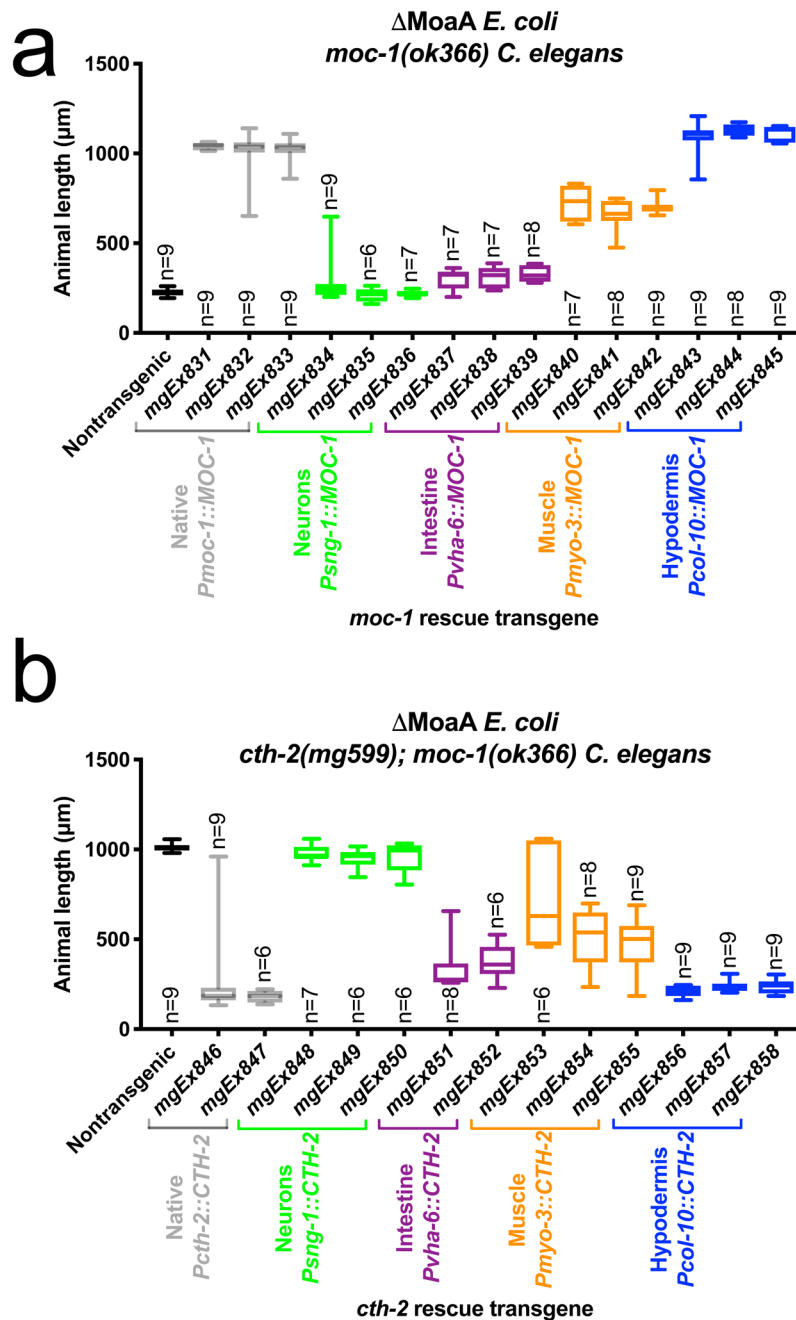


**Figure 6: Tissue specific rescue of *suox-1*, *moc-1*, and *cth-2*.**

(A) Nontransgenic *moc-1(ok366)* and *moc-1(ok366)* transgenic animals expressing *moc-1* under the control of the *moc-1* (native, gray), *sng-1* (neurons, green), *vha-6* (intestine, purple), *myo-3* (muscle, orange), or *col-10* (hypodermis, blue) promoters were cultured for 72 hours from the first larval stage on MoaA mutant *E. coli* and animal lengths were quantified. Each rescue construct was tested with 3 independently isolated transgenes. (B) Nontransgenic *cth-2(mg599); moc-1(ok366)* and *cth-2(mg599); moc-1(ok366)* transgenic animals expressing *cth-2* under the control of the *cth-2* (native, gray), *sng-1* (neurons, green), *vha-6* (intestine, purple), *myo-3* (muscle, orange), or *col-10* (hypodermis, blue)

promoters were cultured for 72 hours from the first larval stage on MoaA mutant *E. coli* and animal lengths were quantified. Each rescue construct was tested with 2–3 independently isolated transgenes. Box plots display the median, upper, and lower quartiles while whiskers indicate minimum and maximum data points. Sample size (n) is the number of individuals assayed and is displayed for each experiment.

Author Manuscript

Author Manuscript

Author Manuscript

Author Manuscript